Contact dynamic phenomena in rotating machines: active/passive considerations

Patrick S. Keogh

Department of Mechanical Engineering, University of Bath, Bath BA2 7AY, UK
E-mail address: enspsk@bath.ac.uk

ABSTRACT
There are machine operating regimes in which rotor/stator interactions may lead to problematic rotor dynamic behaviour. For example, dynamic heat sources arising from seals, bearings and other rubbing stator components may cause rotor thermal bend instability. In active magnetic bearing (AMB) systems, the rotor may experience forward and backward whirl rubs with touchdown bearings (TDBs). In abnormal cases, rotor transient and bounce interactions with such bearings may involve highly localized and short duration contacts. This paper discusses certain contact phenomena that may occur in passive and active systems. For example, the rub induced spiral behaviour arises from a combination of unbalance and a thermal input that moves slowly around the rotor, typically in passive rotor-bearing systems. However, the instability can be regarded as if arising from a closed loop feedback system. Hence it is possible to analyse the phenomenon using techniques that have been developed for active control systems. Rotors levitated by AMBs are truly active, but there are fundamental issues that may arise when contact with TDBs occurs. AMB control and contact interactions are discussed together with the benefits for making the TDB an active element. The reason for this lies in the potential ability to control the contact dynamics and associated mechanical and thermal stresses. A prototype system is described.

Keywords: Rotor/stator contact, thermal bend, touchdown bearings.

1. Introduction

There are many rotating machine types ranging from low to high in terms of rotor size, complexity, operating speed, load/torque, power and rigidity. A rotor may be supported by a range of bearings, passive or active, and it may also interact with seals, brushes and other stator components. The machines may also be mounted on nominally rigid foundations, on flexible structures, or operate in motion based transport environments. Normal design procedures would require that the dynamic stability and response of the system be verified according to particular standards e.g. API [1] or ISO [2]. However, there are occasional instances in which the rotor dynamics differ from the expected behavior due to interactions with stator components. An indication of the problems that may arise from contact events is shown in Fig. 1. In this paper, two cases are considered, namely, rotor thermal bending, and the dynamic contact events that may occur in AMB systems.

The thermal bend problem has received attention from a number of researchers [1-26]. It is generally associated with rotor/stator interactions in which the coupling stresses are relatively small and do not have a significant influence on the usual rotor dynamics. Instead, the main coupling is indirect, through asymmetric rotor heating, leading to a dynamic thermal bend. The early works of Taylor [3], Newkirk [4], and Kroon and Williams [5] identify rub induced bending, now known as the Newkirk effect. Since that time analytical procedures have been developed [6-11]. Other interesting industrial cases that report the problem are given in [12] and [13]. Typically, the friction induced heating arises from seals or slip-ring brushes.

Thermal bending may also arise from other sources including lubricant shearing in a hydrodynamic bearing. Schmied [8] recognized this and further analysis in [14, 15] detailed the

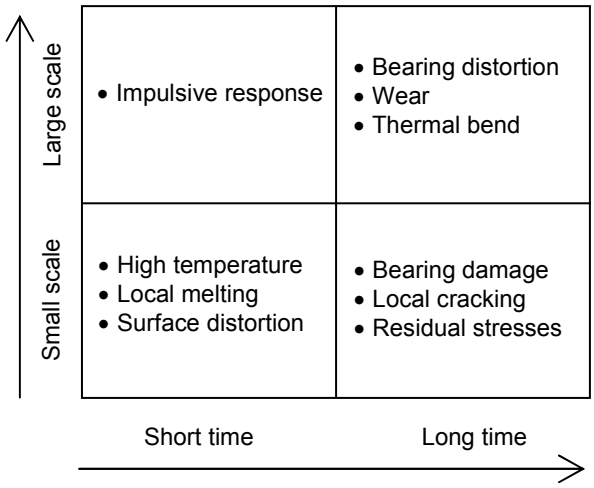

Fig. 1. Scale/time issues for rotor contact

dynamic interaction. This is now known as the Morton effect and has been studied further in [16-25]. Recently, Eldridge *et al.* [26] have reported the effect in a microturbine system with the heat source originating from a rolling element bearing.

In the first part of this paper, an analysis of the thermal bend problem is proposed in the transfer function domain. Such a formulation, which is typically used by control strategy designers, enables the stability of closed loop thermal bending to be assessed from the frequency response of the open-loop transfer function. The thermal bend development is often quoted in terms of "synchronous instability", but in this paper the frequency refers to a perturbation about the synchronous frequency. The Nyquist stability criterion may then be used for stability assessment. It is also possible to specify a bounding expression to guarantee system stability.

The second consideration of the paper relates to the rotor/TDB interaction in AMB systems. In this case, the coupling stresses are sufficiently strong such that the levitated rotor dynamics are changed. A range of analytical procedures and measurement techniques have been considered for the non-linear dynamics associated with a clearance region [27-43]. Specifically, for AMB systems, drop tests have been undertaken by Schmied and Pradetto [44], Kirk *et al*. [45-47], and Hawkins *et al*. [48]. Further comprehensive assessments of TDB dynamics are considered in [49-79]. In most cases, the AMB/TDB interaction is not considered, the problem being a power loss condition with uncontrolled rotor motion. Few papers cover the case when the AMB is still functional. The issues that arise relate to instability caused by the change in the plant dynamics, for which the AMB control strategy may be inappropriate. Also, the co-existence of a normally levitated contact-free rotor dynamic response and trapped modes involving persistent contact may require additional control action. For a common unbalance condition it is desirable to have stable contact-free dynamics, but unsustainable trapped contact modes. The paper will report on current progress in the development of active TDBs to destabilize trapped contact modes [80-83].

2. Dynamics of thermal bending

The intention is to formulate the thermal bend problem in terms of transfer function relations, where time variations are represented in the Laplace transform domain. A transfer function simply relates the input and output in an algebraic sense. With appropriate choice of the Laplace transform variable, the frequency response is readily obtained. This approach contrasts with the direct time

formulation of the thermal input as proposed by Kellenberger [7], or recently by Bachschmid *et al*. [11].

2.1. Imposed harmonic motion

The rotor dynamics are not considered to be influenced directly by the forces or stresses arising from the contact. Instead the heat generation from the contact causes a rotor thermal bend to develop (Fig. 2), which changes the unbalance distribution. The starting point of the analysis is to assume that a steady, harmonic, not necessarily synchronous, linearized rotor dynamic motion (elliptical) is applied at a rotor axial location where stator interaction can occur.

2.2. General harmonic heat input

The imposed harmonic rotor motion is considered to be at the perturbed non-synchronous frequency $\varpi = \Omega + \omega$, where Ω is the rotational frequency and ω is the perturbation. As a result of rotor/stator interaction, the rotor will experience a heat input that is periodic at frequency ϖ. Hence it is generally possible to decompose the surface heat flux input into double Fourier series

$$Q(\theta, z, t) = \sum_{m=-\infty}^{\infty} \sum_{n=-\infty}^{\infty} q_{mn}(z) e^{i(n\theta + m\varpi t)} \tag{1}$$

Here θ and z are circumferential and axial coordinates, respectively, referred to a stationary reference frame (Fig. 2). To examine heat conduction in the rotor it is appropriate to refer the circumferential coordinate to synchronously rotating axes (u, v):

$$\theta = \beta + \Omega t \tag{2}$$

Then the heat input transforms to $Q(\beta + \Omega t, z, t) = q(\beta, z, t)$, where

$$q(\beta, z, t) = \sum_{m=-\infty}^{\infty} \sum_{n=-\infty}^{\infty} q_{mn}(z) e^{i(n\beta + (m\varpi + n\Omega)t)} \tag{3}$$

This will cause a temperature distribution to be set up in the rotor section around the contact zone. This temperature is a relatively straightforward solution of a dynamic conduction problem within the rotor section, subject to appropriate thermal boundary conditions. It may be formulated in the Laplace transform domain. Omitting details the thermal response will take the form

$$\begin{aligned} \widetilde{q}(\beta, z, s) &= \sum_{n=-\infty}^{\infty} \widetilde{q}_n(z, s) e^{in\beta} \\ \widetilde{T}(r, \beta, z, s) &= \sum_{n=-\infty}^{\infty} \frac{\widetilde{q}_n(z, s)}{h_n(r, z, s)} e^{in\beta} \end{aligned} \tag{4}$$

where $T(r, \beta, z, t)$ is the rotor section temperature, r is a radial coordinate, s the Laplace transform variable, and $\widetilde{\ }$ denotes the Laplace transform. Also, $h_n(r, z, s)$ is a spatial harmonic heat transfer function. For the specified harmonic heat input it is a simple matter to deduce that

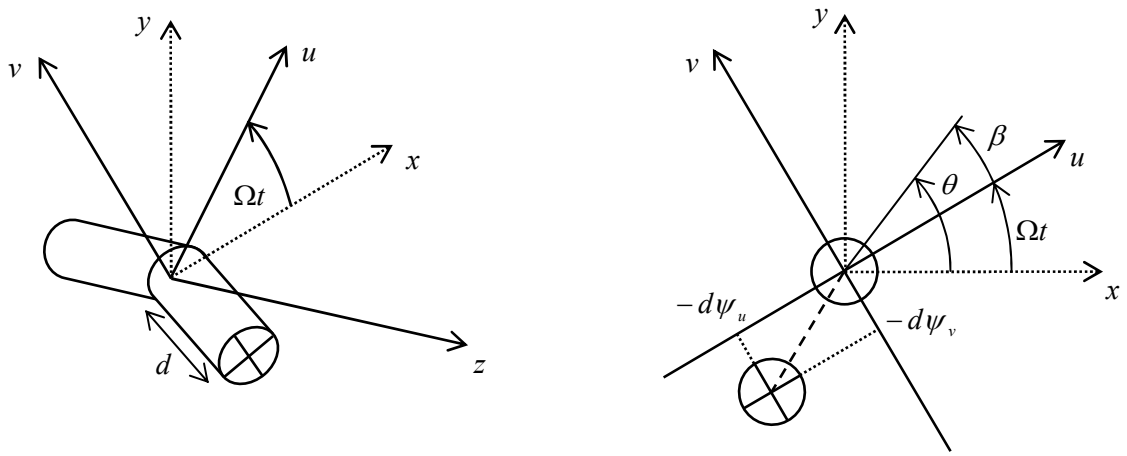

Fig. 2. Rotor section bend definition referred to a synchronously rotating reference frame

$$\tilde{q}_n(z,s) = \sum_{m=-\infty}^{\infty} \frac{q_{mn}(z)}{s - i(m\varpi + n\Omega)} \tag{5}$$

In the time domain, the developed temperature is given by

$$T(r,\beta,z,t) = \sum_{m=-\infty}^{\infty} \sum_{n=-\infty}^{\infty} T_n(r,z,m\varpi + n\Omega) e^{i(n\beta + (m\varpi + n\Omega)t)} \tag{6}$$

where

$$T_n(r,z,m\varpi + n\Omega) = \frac{q_{mn}(z)}{h_n(r,z,i(m\varpi + n\Omega))} \tag{7}$$

2.3. Thermal bend evaluation

To evaluate the thermal bend for a fully developed rotor temperature distribution, only the temperature component associated with the first spatial harmonic ($n = -1$) is required (Dimarogonas, [6]). The time dependent bend angle components $(\psi_u(t), \psi_v(t))$ are referred to the synchronously rotating axes (u, v) as shown in Fig. 2. For a solid rotor section they may be evaluated in the complex form:

$$\begin{aligned} \psi(t) &= \psi_u(t) + i\psi_v(t) \\ &= \frac{2\alpha}{I} \int_0^R \int_0^{2\pi} \int_0^{L_S/2} r^2 T(r,\beta,z,t) e^{i\beta} dz d\beta dr \\ &= \frac{4\pi\alpha}{I} \sum_{m=-\infty}^{\infty} \int_0^R \int_0^{L_S/2} r^2 T_{-1}(r,z,m\varpi - \Omega) dz dr e^{i(m\varpi - \Omega)t} \end{aligned} \tag{8}$$

Here, α is the thermal expansion coefficient, I is the second moment of area, R is the radius and L_S is a suitably large length of rotor section surrounding the contact zone. This expression may be rearranged to enable the complex bend angle to be composed of time harmonics:

$$\psi(t) = \psi_0(\omega)e^{i\omega t} + \sum_{\substack{l=-\infty \\ l\neq 0}}^{\infty} \psi_l(\omega_l)e^{i\omega_l t} \tag{9}$$

where $\omega_l = l\Omega + (l+1)\omega$ and

$$\psi_l(\omega_l) = \frac{4\pi\alpha}{I}\int_{R_i}^{R_o}\int_0^{L_S/2} r^2 T_{-1}(r,z,\omega_l)\,dz\,dr \tag{10}$$

The first term $(l = m-1 = 0)$ becomes stationary when $\omega = \omega_0 = 0$, which corresponds with the purely synchronous orbit case of $\varpi = \Omega$. It is to be expected from the thermal conduction problem that a significant and developed temperature difference across the rotor will only occur at slow timescales when ω is relatively small. Other stationary bend conditions occur when $\omega_l = 0$ i.e. $\omega = -l\Omega/(l+1)$, but these are not considered to be typical of those arising from rub type contacts. Hence the bend expression is simplified to

$$\psi(t) = \psi_0(\omega)e^{i\omega t} \tag{11}$$

It is also possible to use equations (4) and (8) to determine the Laplace transformed version of the bend angle as

$$\tilde{\psi}(s) = \frac{4\pi\alpha}{I}\int_0^{R}\int_0^{L_S/2} r^2\,\frac{\tilde{q}_{-1}(z,s)}{h_{-1}(r,z,s)}\,dz\,dr \tag{12}$$

The complex amplitude in equation (11) follows from the frequency response evaluation:

$$\psi_0(\omega) = \frac{4\pi\alpha}{I}\int_0^{R}\int_0^{L_S/2} r^2\,\frac{q_{1,-1}(z)}{h_{-1}(r,z,i\omega)}\,dz\,dr \tag{13}$$

2.4. Orbit – thermal bend relation

Let (x, y) be the fixed frame coordinates of the rotor section center of mass. In complex notation,

$$z = x + iy = z_0 + z_E \tag{14}$$

where $z_0 = x_0 + iy_0$ is a static offset. For an elliptical orbit, regarded as a combination of circular whirls,

$$z_E = x_E + iy_E = \varepsilon_B e^{-i(\varpi t-\varphi)} + \varepsilon_F e^{i(\varpi t+\varphi)} \tag{15}$$

where ε_B is the circular backward whirl radius, ε_F is the circular forward whirl radius, and φ is a phase angle.

As the orbit is traversed, the rotor may experience variable contact conditions with a stator component. A linearization argument can be used to express the heat input as a steady component due to the static offset, together with dynamic components due to the whirl combination:

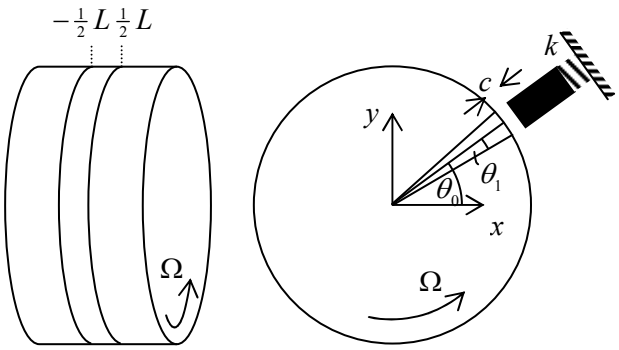

Fig. 3. Rotor section and possible contact with a friction element

$$Q(\theta,z,t) = Q_0(\theta,z) + \varepsilon_B Q_B(\theta,z,t) + \varepsilon_F Q_F(\theta,z,t) \tag{16}$$

Since the first term is steady, no significant thermal bend can arise. The general elliptic orbit will therefore give rise to a complex bend angle of the form

$$\psi(t) = \varepsilon_B \psi_B(t) + \varepsilon_F \psi_F(t) \tag{17}$$

where $\psi_{\{B,F\}}(t) = \psi_{\{B,F\}0}(\omega)e^{i\omega t}$. Here $\psi_{\{B,F\}0}(\omega)$ may be evaluated from the corresponding rotor thermal conduction problems due to the heat inputs associated with backward and forward whirls.

It is desirable for rotor dynamic analysis purposes to relate the thermal bend amplitude $\psi_0(\omega)$ angle to complex rotor displacement harmonic amplitudes, $Z_{X,Y}(\varpi)$, in the fixed axis system:

$$\begin{aligned} x_E &= x_B + x_F = \mathrm{Re}\{Z_X(\varpi)e^{i\varpi t}\} \\ y_E &= y_B + y_F = \mathrm{Re}\{Z_Y(\varpi)e^{i\varpi t}\} \end{aligned} \tag{18}$$

Comparing equations (15) and (18), the backward and forward orbit radii are related to the complex amplitudes by

$$\begin{aligned} \varepsilon_B &= \tfrac{1}{2}(Z_X(\varpi) - iZ_Y(\varpi))e^{i\varphi} \\ \varepsilon_F &= \tfrac{1}{2}(Z_X(\varpi) + iZ_Y(\varpi))e^{-i\varphi} \end{aligned} \tag{19}$$

The phase angle φ is arbitrary and may be set to zero without loss of generality. It is therefore deduced that the complex thermal bend amplitude is related to the complex displacement amplitudes according to

$$\psi_0(\omega) = B_{TX}(\omega)Z_X(\varpi) + B_{TY}(\omega)Z_Y(\varpi) \tag{20}$$

where the coefficients are given by

$$\begin{aligned} B_{TX}(\omega) &= \tfrac{1}{2}(\psi_{B0}(\omega) + \psi_{F0}(\omega)) \\ B_{TY}(\omega) &= -\tfrac{1}{2}i(\psi_{B0}(\omega) - \psi_{F0}(\omega)) \end{aligned} \tag{21}$$

Relation (20) shows how input displacement amplitudes of frequency ϖ transfer to an output thermal bend amplitude with frequency ω. An appropriate transfer function relation corresponding to (20) has the form

$$\tilde{\psi}(s) = G_{TX}(s+i\Omega)\tilde{x}_E(s+i\Omega) + G_{TY}(s+i\Omega)\tilde{y}_E(s+i\Omega) \tag{22}$$

This will provide the frequency response of equation (20) if

$$\begin{aligned} B_{TX}(\omega) &= G_{TX}(i\varpi) = G_{TX}(i(\omega+\Omega)) \\ B_{TY}(\omega) &= G_{TY}(i\varpi) = G_{TY}(i(\omega+\Omega)) \end{aligned} \tag{23}$$

2.5. Heat input example

Consider a rotor that may come into contact with a simple spring mounted friction element (Fig. 3), with possible contact over the arc $\theta_0 - \theta_1 \le \theta \le \theta_0 + \theta_1$ and axial strip $-L/2 \le z \le L/2$. Suppose that the rotor undergoes an imposed harmonic displacement

$$x = X\sin\varpi t \tag{24}$$

If the clearance is exceeded $(X\cos\theta_0 > c)$ then contact will occur over some time interval $T_0 - T_1 < t < T_0 + T_1$ within the first cycle and periodically thereafter. For the zero clearance ($c = 0$) case, $T_0 = T_1 = \pi/2\varpi$ i.e. contact will occur over half of the displacement cycle. The spring deflection will cause a variation in the normal contact force, hence also of friction and the heat dissipation rate. If the heat is generated from uniform contact and all of it enters the rotor then

$$Q(\theta, z, t) = Q_X X\sin\varpi \tag{25}$$

whenever $\theta_0 - \theta_1 \le \theta \le \theta_0 + \theta_1$ and $0 < t < \pi/\varpi$, otherwise the heat input is zero. Here, $Q_X = \mu\Omega k\cos\theta_0 / 2\theta_1 L$ where μ is the coefficient of friction and k is the spring stiffness. A double Fourier series decomposition leads to the $m = 1, n = -1$ coefficient

$$q_{1,-1} = -\frac{Q_X e^{i\theta_0}\sin\theta_1}{4\pi\varpi} Z_X(\varpi) \tag{26}$$

since $Z_X(\varpi) = -iX$ is the complex harmonic amplitude. The thermal conduction solution now yields

$$B_{TX}(\omega) = -\frac{\alpha Q_X e^{i\theta_0}\sin\theta_1}{I\varpi}\int_0^R\int_0^{L_S/2}\frac{r^2}{h_{-1}(r,z,i\omega)}\,dzdr \tag{27}$$

A similar procedure can be adopted to determine

$$B_{TY}(\omega) = -\frac{\alpha Q_Y e^{i\theta_0}\sin\theta_1}{I\varpi}\int_0^R\int_0^{L_S/2}\frac{r^2}{h_{-1}(r,z,i\omega)}\,dzdr \tag{28}$$

where $Q_Y = \mu\Omega k\sin\theta_0 / 2\theta_1 L$. Equivalent transfer function relations as appearing in equation (22) are

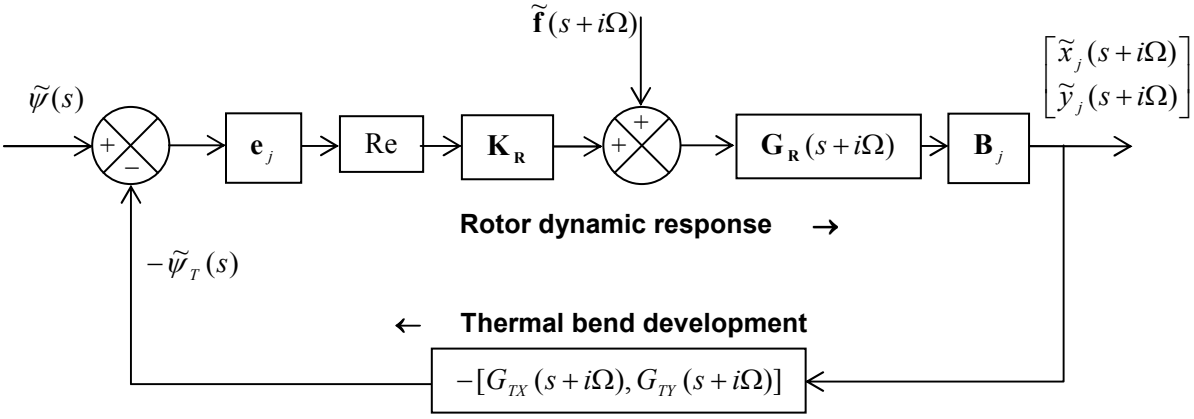

Fig. 4. Closed loop system indicating thermal bend/rotor dynamic interaction

$$G_{T\{X,Y\}}(s+i\Omega) = -i\frac{\alpha Q_{\{X,Y\}} e^{i\theta_0}\sin\theta_1}{I(s+i\Omega)}\int_0^R\int_0^{L_S/2}\frac{r^2}{h_{-1}(r,z,s)}\,dzdr \tag{29}$$

In this example, the heat input is zero for the half cycle in which contact does not occur. If the spring were to be preloaded such that contact was never lost, it is simply the case that the bend angle coefficients would be scaled by a factor of 2. It is also remarked that other sources of heat, such as those due to an oscillating hydrodynamic bearing oil film, may also be analyzed using the relation (22).

2.6. Rotor dynamic response from bend input

The general linearized form of the rotor dynamic equation of motion for a straight discretized rotor may be written as

$$\mathbf{M}_\mathbf{R}\ddot{\mathbf{r}} + (\mathbf{C}_\mathbf{B} + \Omega\mathbf{I}_\mathbf{R})\dot{\mathbf{r}} + (\mathbf{K}_\mathbf{B} + \mathbf{K}_\mathbf{R})\mathbf{r} = \mathbf{f} \tag{30}$$

where $\mathbf{r} = [\mathbf{r}_\mathbf{x}^T, \mathbf{r}_\mathbf{y}^T]^T$, such that the $x-z$ and $y-z$ plane generalized lateral deflection (translation and angle) coordinates of the rotor are separated into

$$\begin{aligned}\mathbf{r}_\mathbf{x} &= [x_1, \vartheta_1, x_2, \vartheta_2, \ldots, x_N, \vartheta_N]^T\\ \mathbf{r}_\mathbf{y} &= [y_1, \phi_1, y_2, \phi_2, \ldots, y_N, \phi_N]^T\end{aligned} \tag{31}$$

Also, $\mathbf{f}$ contains the corresponding generalized external forces, and $\{\mathbf{M}_\mathbf{R}, \mathbf{I}_\mathbf{R}, \mathbf{C}_\mathbf{B}, \mathbf{K}_\mathbf{B}, \mathbf{K}_\mathbf{R}\}$ are associated mass, inertia, damping and stiffness matrices associated with the rotor (R) and bearings (B).

Consider now the rotor to be bending, say at node *j*, with a complex bend angle $\psi(t)$. The total rotor deflection from the unbent rotor equilibrium line can be expressed in the form $\mathbf{r} = \mathbf{r}_\psi + \mathbf{r}_\delta$, where $\mathbf{r}_\psi$ defines the bent shape and $\mathbf{r}_\delta$ is due to dynamic lateral deflection. The rotor dynamic equation then becomes

$$\mathbf{M}_\mathbf{R}\ddot{\mathbf{r}} + (\mathbf{C}_\mathbf{B} + \Omega\mathbf{I}_\mathbf{R})\dot{\mathbf{r}} + \mathbf{K}_\mathbf{B}\mathbf{r} + \mathbf{K}_\mathbf{R}\mathbf{r}_\delta = \mathbf{f} \tag{32}$$

since rotor strain energy depends only on $\mathbf{r}_\delta$. A simple manipulation then gives

$$\mathbf{M_R}\ddot{\mathbf{r}} + (\mathbf{C_B} + \Omega\mathbf{I_R})\dot{\mathbf{r}} + (\mathbf{K_B} + \mathbf{K_R})\mathbf{r} = \mathbf{f} + \mathbf{K_R}\mathbf{r}_\psi \tag{33}$$

With reference to Fig. 2, the a local bend will cause a section of rotor of length d to deviate by

$$u + iv = -d\psi(t) \tag{34}$$

in complex synchronously rotating coordinates. In fixed coordinates, this is transformed to

$$x + iy = -d\psi(t)e^{i\Omega t} \tag{35}$$

It follows that the bent shape component can be expressed in the form

$$\mathbf{r}_{\psi\mathbf{x}} + i\mathbf{r}_{\psi\mathbf{y}} = \mathbf{d}_j\psi(t)e^{i\Omega t} \tag{36}$$

Here $\mathbf{d}_j$ is a vector of the form

$$\mathbf{d}_j = [0,0,\ldots,0,0,-d_j,-1,\ldots,-d_N,-1]^T \tag{37}$$

where $d_j = l_j, d_{j+1} = l_j + l_{j+1}, \ldots, d_N = l_j + \ldots + l_N$ are axial distances of element nodes from the bend location. This implies that $\mathbf{r}_\psi = \mathrm{Re}\{\mathbf{e}_j\psi(t)e^{i\Omega t}\}$ with $\mathbf{e}_j = [\mathbf{d}_j^T, -i\mathbf{d}_j^T]^T$. It now follows that $\mathbf{r} = \mathrm{Re}\{\mathbf{z}\}$ follows by solving

$$\mathbf{M_R}\ddot{\mathbf{z}} + (\mathbf{C_B} + \Omega\mathbf{I_R})\dot{\mathbf{z}} + (\mathbf{K_B} + \mathbf{K_R})\mathbf{z} = \mathbf{f} + \mathbf{K_R}\mathbf{e}_j\psi(t)e^{i\Omega t} \tag{38}$$

In terms of the Laplace transform, the solution is

$$\tilde{\mathbf{z}}(s) = \mathbf{G_R}(s)\tilde{\mathbf{f}}(s) + \mathbf{G_R}(s)\mathbf{K_R}\mathbf{e}_j\tilde{\psi}(s - i\Omega) \tag{39}$$

where $\mathbf{G_R}(s) = (s^2\mathbf{M_R} + s(\mathbf{C_B} + \mathbf{\Omega I_R}) + (\mathbf{K_B} + \mathbf{K_R}))^{-1}$.

The corresponding components associated with the rotor displacements at the bend location may be extracted using an appropriate transformation matrix $\mathbf{B}_j$. By also adjusting the Laplace transform variable, the orbit at the bend location is expressible as

$$\begin{bmatrix} \tilde{x}_j(s + i\Omega) \\ \tilde{y}_j(s + i\Omega) \end{bmatrix} = \mathbf{B}_j\mathbf{G_R}(s + i\Omega)\tilde{\mathbf{f}}(s + i\Omega) + \mathbf{B}_j\mathbf{G_R}(s + i\Omega)\mathbf{K_R}\ \mathrm{Re}(\mathbf{e}_j\tilde{\psi}(s)) \tag{40}$$

2.7. Rotor dynamic/thermal bend coupling and stability

Thus far, open-loop relations have been deduced for the thermal bend/orbit response and the orbit/thermal bend response. It is now a simple matter to couple these relations to form the closed loop system shown in Fig. 4. This form may be conveniently assessed using control theory techniques for stability and simulation purposes. The open-loop transfer function relation from the left hand side bend angle input to the evaluated thermal bend is

$$\widetilde{\psi}_T(s) = [G_{TX}(s+i\Omega), G_{TY}(s+i\Omega)]\,\mathbf{B}_j\mathbf{G}_\mathbf{R}(s+i\Omega)\mathbf{K}_\mathbf{R}\ \mathrm{Re}(\mathbf{e}_j\widetilde{\psi}(s)) \tag{41}$$

In terms of the frequency response, the relevant relation is

$$\psi_{T0}(\omega) = [B_{TX}(\omega), B_{TY}(\omega)]\mathbf{B}_j\mathbf{G}_\mathbf{R}(i\varpi)\mathbf{K}_\mathbf{R}\ \mathrm{Re}(\mathbf{e}_j\psi_0(\omega)) \tag{42}$$

In fact, the input bend can be arbitrarily chosen and if it is selected to be the real component $\psi(t) = \psi_u(t)$, it follows that the frequency response relation is

$$\frac{\psi_{T0}(\omega)}{\psi_{u0}(\omega)} = [B_{TX}(\omega), B_{TY}(\omega)]\mathbf{B}_j\mathbf{G}_\mathbf{R}(i\varpi)\mathbf{K}_\mathbf{R}\begin{bmatrix}\mathbf{d}_j\\ \mathbf{0}\end{bmatrix} \tag{43}$$

This is now in the classic form for a Nyquist criterion assessment of the closed loop system. It states that if the locus of the open-loop frequency response $-\psi_{T0}(\omega)/\psi_{u0}(\omega)$ in the complex plane does not encircle the point -1, then the closed loop system will be stable. Equivalently, $\psi_{T0}(\omega)/\psi_{u0}(\omega)$ should not encircle the point 1 for stability. A conservative condition for stability is to require the locus of $\psi_{T0}(\omega)/\psi_{u0}(\omega)$ to remain within the unit circle, which will be the case if

$$\left|\frac{\psi_{T0}(\omega)}{\psi_{u0}(\omega)}\right| \le \bar{\sigma}([B_{TX}(\omega), B_{TY}(\omega)])\bar{\sigma}(\mathbf{B}_j\mathbf{G}_\mathbf{R}(i\varpi))\bar{\sigma}(\mathbf{K}_\mathbf{R}[\mathbf{d}_j^T, \mathbf{0}^T]^T) < 1 \tag{44}$$

where $\bar{\sigma}$ denotes the largest singular value of each considered matrix. Specifically,

$$\begin{aligned}\bar{\sigma}([B_{TX}(\omega), B_{TY}(\omega)]) &= \sqrt{|B_{TX}(\omega)|^2 + |B_{TY}(\omega)|^2}\\ \bar{\sigma}(\mathbf{K}_\mathbf{R}[\mathbf{d}_j^T, \mathbf{0}^T]^T) &= F_{\mathrm{R}j}\end{aligned} \tag{45}$$

The latter expression for $F_{\mathrm{R}j}$ provides a measure of the rotor forces and moments that would be required to statically restore the rotor to a perfectly straight state from a bent condition with a unit bend angle. Finally, the rotor dynamics are captured by the term $\bar{\sigma}(\mathbf{B}_j\mathbf{G}_\mathbf{R}(i\varpi))$. It is remarked that Cloud *et al*. [84] have previously considered singular value decomposition applications in rotor dynamics. The specified criterion for stability embeds the combination of influences that should be considered to ensure that unstable thermal bending does not occur. Thus a large rotor dynamic response may require the thermal input driver to be reduced. The value of $F_{\mathrm{R}j}$ determines the overall sensitivity through the axial location of the thermal source. As with modern control specifications of stability, the condition (44) is conservative. Hence, if it is not satisfied, stability may still apply, but the Nyquist criterion should be invoked for a definitive stable/unstable result.

3. Rotor/touchdown bearing issues

An active magnetic bearing (AMB) system typically has an associated touchdown bearing (TDB) system to deal with abnormal operating conditions that would otherwise lead to rotor/AMB stator contact. The TDBs are designed to be capable of enduring a number of rotor drops and run-downs, though this can be quite low in practice [72-74]. Such a condition involves a non-operational AMB system, resulting in rotor de-levitation and contact with the TDBs [44-48]. One of the main objectives is to avoid the large contact forces associated with rotor backward whirl. Braking may be applied to

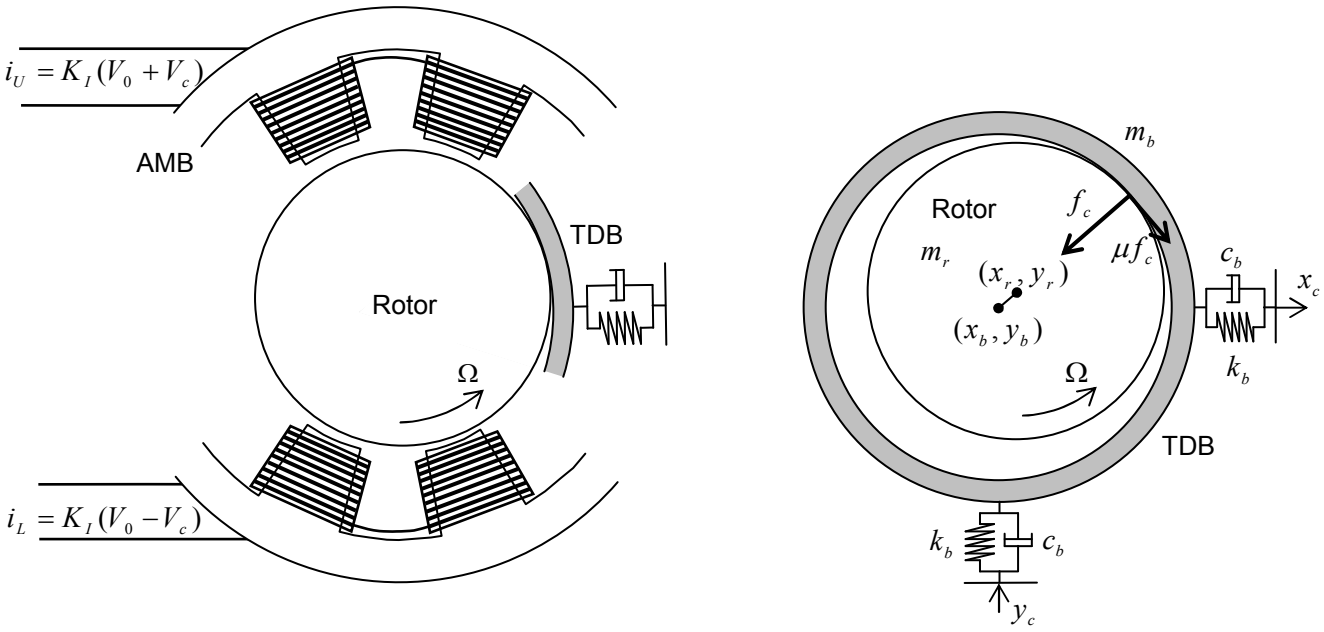

Fig. 5. Schematic of rotor/AMB/TDB showing possible rotor/TDB contact

the rotor to reduce run-down times and prevent excessive vibration amplitudes on passing through rotor-on-TDB critical speeds.

In contrast with the de-levitation case, there are relatively few papers that deal with the contact problem with a fully operational AMB system. In this case, rotor/TDB contact may occur if there is an intermittent fault, or if there is a sufficiently high lateral acceleration input through the AMBs. Often AMBs are configured to transmit low forces at an operating speed, with a low dynamic stiffness, achieved using a notch filter in the control loop. Such a configuration would be prone to the acceleration input problem and also AMB control induced instability due to a change in the plant dynamics under contact conditions. It is conceivable to design controllers that "stiffen" the AMBs when acceleration inputs occur. However, bandwidth and load capacity limitations suggest that it is unrealistic to expect this approach to prevent rotor/TDB contact completely.

In this section, the issues associated with levitated rotor/TDB contact will be highlighted. It will be indicated that the rotor may exist in a normal contact-free levitated condition, or in a number of limit cycle trapped contact modes. Unless action is taken the trapped modes may persist. In such cases the contact forces, which are essentially unbalance driven, may become excessively large. Furthermore, bounce-like contact events may give rise to highly localized mechanical and thermal stresses. The options for using AMB control and active TDB control will be discussed. In practice, an active TDB will be feasible only if the necessarily demanding control forces can be applied effectively. Hence, the case is limited to relatively small rotor systems.

3.1. Consequences of rotor/TDB contact

Figure 5 shows an arrangement of a radial AMB/TDB system in which the rotor/TDB clearance c_{rb} will be lower than the rotor/AMB clearance c_{ra}. Under normal operation, the AMB control currents will maintain the rotor within the available clearance space. For an unbalanced rigid rotor it is common to allow it to spin about the principal axis to minimize transmitted forces through the AMB. In other cases, more precise rotor position control may be achieved, though at the expense of increased transmitted forces. These characteristics may be implemented through the control strategy design,

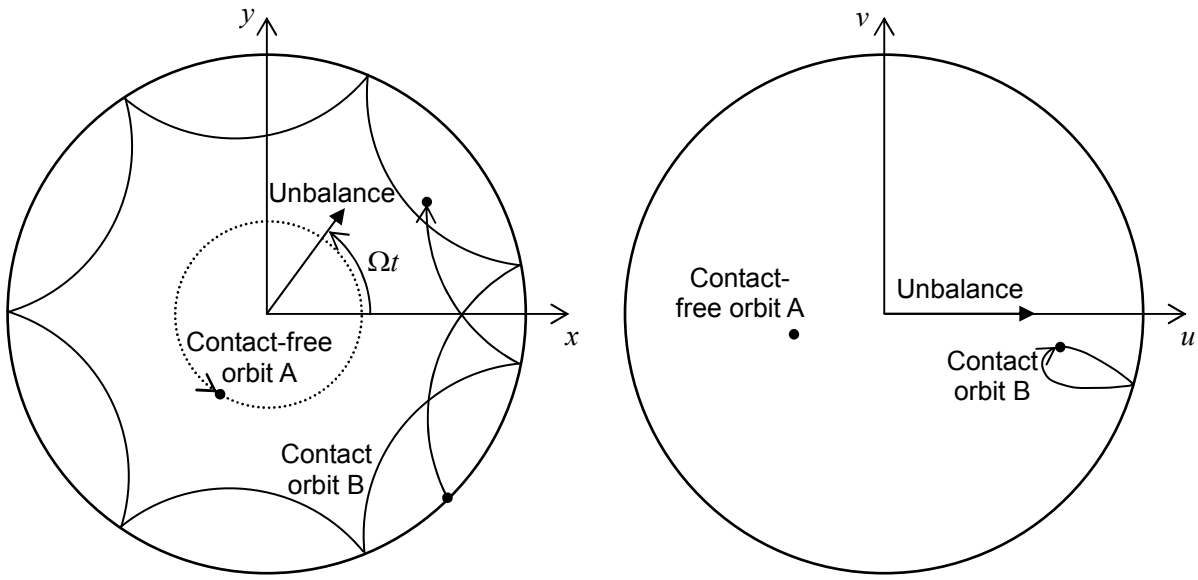

Fig. 6. Co-existence of a contact-free orbit A and an orbit involving periodic contact B. The left diagram shows the orbits in a stationary reference frame (x, y), while the right diagram shows the same information in a synchronously rotating reference frame (u, v)

which would utilize rotor position sensor measurements to evaluate appropriate amplifier signals, hence to drive the AMB coil currents.

It is assumed that the AMB is operational, but due to some intermittent fault or transient input, the rotor (mass m_r) makes contact with the TDB (mass m_b) as shown in Fig. 5. The TDB is assumed to be mounted with an effective radial stiffness k_b and damping c_b combination. The rotor displacement is denoted by (x_r, y_r) and the TDB displacement by (x_b, y_b). If the relative displacement between the rotor and TDB centers exceeds the radial clearance c_{rb}, contact must occur resulting in the normal force f_c and friction force μf_c. The TDB becomes an active element if the displacement (x_c, y_c) is imposed by external excitation. For a passive system this displacement is set to zero.

3.2. Idealized bounce/rub contact

Idealized bounce-like contact events may be represented by contact forces that are impulsive, leading to an instantaneous change of rotor momentum. The impulsive nature of the contact force means that the parameters associated with the TDB are not considered. It is possible to seek for periodic solutions that are stable in the sense that contacts persist [64, 65]. They are driven by the rotor unbalance condition and Fig. 6 gives a pictorial representation of the type of solution that is possible (orbit B). Orbit A is the corresponding non-contacting response i.e. the circular orbit within the clearance space assuming linear isotropic AMB characteristics. Orbits A and B may be represented in stationary (x, y) and synchronously rotating (u, v) reference frames. The synchronous frame view is informative in that it provides phase change information for the orbits relative to the unbalance. When applied to a system with parameters as in Table 1, multiple contact solutions are obtained (Fig. 7). It is also possible to undertake a force balance for continuous and synchronous circular rub orbits and these are represented by C1 and C2 in Fig. 7. Evidently, these are the continuous equivalents of the impulsive bounce solutions B1 and B4.

The other well-known continuous contact condition not shown in either of Figs 6 or 7 is the

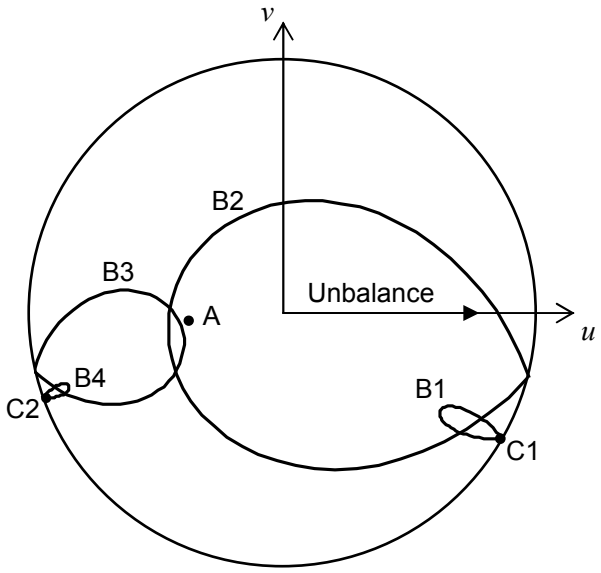

Fig. 7. Synchronous coordinate plot of contact-free orbit (A), contact orbits (B1 … B4), and continuous rub orbits (C1, C2)

backward whirl case involving rolling contact on the TDB. In pure rolling contact, the frequency of the backward whirl is

$$\omega = \left(\frac{R_b}{c_{rb}} \right) \Omega \tag{46}$$

which will be significantly higher than the synchronous frequency Ω (e.g. by a factor above 30 for the data of Table 1). The contact force will greatly exceed the existing synchronous unbalance force and is approximately given by

$$f_c = m_r c_{rb} \omega^2 = m_r c_{rb} \left(\frac{R_b}{c_{rb}} \right)^2 \Omega^2 \tag{47}$$

In practice, this value would be so large that the integrity of the TDB would be in doubt.

Table 1
System data.

Rotor data	m_r = 3.25 kg, R_r = 15.0 mm, e = 0.15 mm Material: steel
AMB data	c_{ra} = 0.8 mm, 8-poles Control: PID ω_n = 300 rad/s, ξ = 0.2 (radial)
TDB data	m_b = 0.18 kg, c_b = 2500 Ns/m, k_b = 6×10^7 N/m R_b = 15.5 mm, L_b = 10.0 mm, c_{rb} = 0.5 mm, μ = 0.05 Type: ball bearing
Speed	Ω = 1000 rad/s (max)

It is possible to examine the stability of the solutions of Fig. 7 by considering velocity perturbations at successive contacts. If the velocity perturbation decreases, the contact orbit is sustainable. A sustainable contact orbit may be termed as a trapped contact mode. In Fig. 7, orbits B1 and B2 (and C1) are trapped contact modes, while B3 and B4 (and C2) are unstable contact orbits. For a simple explanation, the contact-free forced response (A) indicates a near 180 deg phase lag relative to the unbalance forcing, indicating a "soft" AMB stiffness characteristic. When contact conditions apply, the "hard" TDB boundary becomes dominant and is agreeable with the more in-phase trapped modes of B1, B2 and C1.

The rotor dynamics will be expected to behave according to the following cases:

1.1. Remain in a trapped contact mode.
1.2. Transform from an unsustainable contact orbit to a trapped contact mode.
1.3. Transform from an unsustainable contact mode to a backward whirl contact mode.
1.4. Remain in a transitional condition between unsustainable contact modes.
1.5. Move from an unsustainable contact mode to a contact-free orbit of type A.

3.3. Contact zone deformation

The impulsive contact force analysis of the previous section gives some insight into the nature of the contact rotor dynamics, but the TDB mounting characteristics and material properties were not used. It is possible to include a deformable contact zone model e.g. based on a Hertzian stress distribution for simulation purposes. This enables the contact force to be predicted as a function of the penetration depth between the contacting bodies. Energy losses due to contact may be incorporated using a restitution coefficient. Other models are possible that may deal with near conforming contacts [52].

3.4. Thermal issues

There are surprisingly few contributions to the thermal evaluation of rotor/TDB interactions in the open literature. Ohura *et al*. [73] and Reitsma [74] identify the issues associated with thermal heating in TDBs. Development in the air foil bearing area is given by Salehi *et al*. [75]. More typically, TDBs are based on dry bush or rolling element bearing designs with special material properties. Sun *et al*. [76-78] consider a bulk power loss model and a heat transfer network. When a rotor makes initial contact with a stationary TDB, the high contact surface stresses are combined with high slip over a localized contact zone. The rotor and TDB temperatures may be very high, transient and localized within skin depth regions below surfaces. If the contact event is of short duration, or the slip conditions reduce, the heat will generally dissipate in a conductive manner [79].

It is commented that the thermal behavior associated with the thermal bend problem could also exhibit localized and transient characteristics. However, localized temperatures will not give rise to significant thermal bends. These will only develop when heat has been conducted across the rotor section i.e. the temperature is no longer local to the contact zone. The issue for TDBs is the severity of the local temperature due to the potentially high contact forces.

3.5. Flexible rotor systems

The results presented to date are typically associated with rigid rotor systems. However, work on flexible rotor systems has been reported [53, 58, 65]. The added complexity of including flexural modes with the contact dynamics should also be addressed for systems that are considered as having

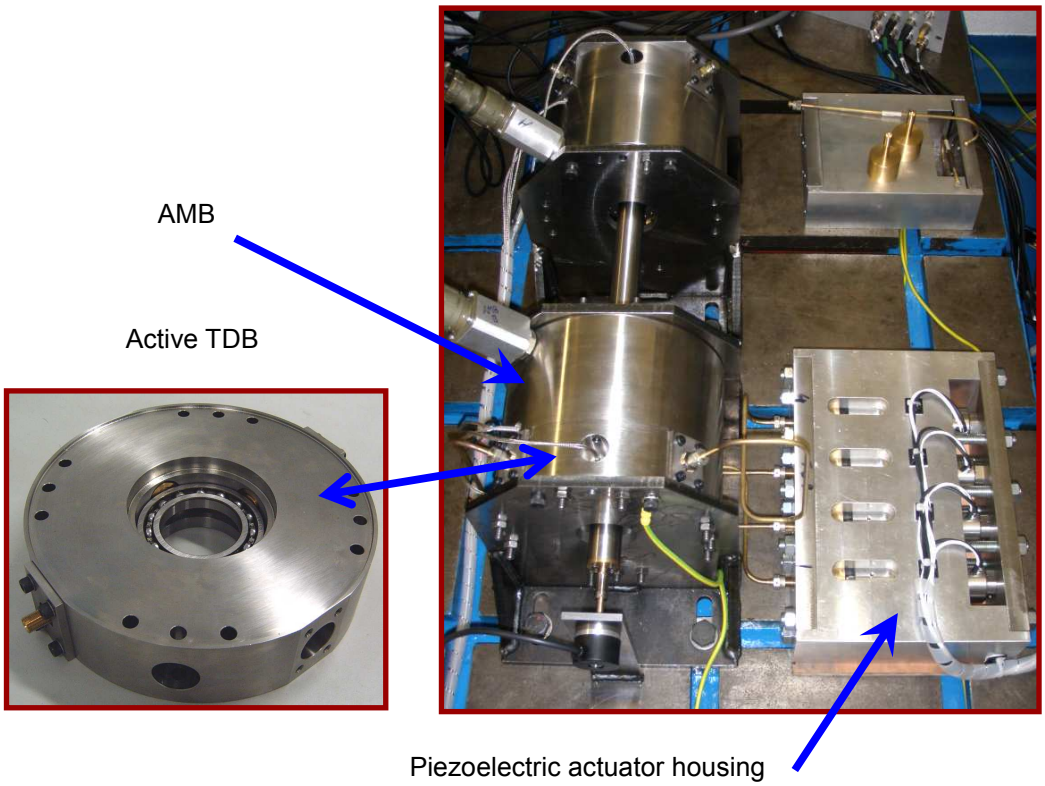

Fig. 8. Active TDB/AMB prototype system

rigid rotors since there will be energy flow paths into flexural modes.

3.6. AMB control options

If an AMB system is still functional, it is natural to question whether the available control potential may be used to alleviate the rotor/TDB contact dynamics. The following points may be raised:

2.1. It is feasible to vary the AMB closed loop radial characteristics on-line. This may have the effect of destabilizing periodic trapped modes involving significant bounce-like behavior within the clearance space. However, rub modes involving only small radial variations may not be significantly affected.

2.2. Periodic trapped modes are driven by the synchronous unbalance. Hence synchronous radial control forces applied by the AMB may reduce the overall driving force to a level at which the trapped mode is not sustainable. The AMB force must be phased correctly and a standard contact-free automatic balancing algorithm may not suffice. From Fig. 7, a standard algorithm would apply trial forces and measure rotor displacement to locate the phase of the unbalance relative to the phase of A. However, if this was attempted for orbits B1, B2 or C1, the unbalance phase would be incorrectly placed. Either the unbalance should be assessed before any conceivable contact or else the algorithm should be adapted for contact dynamic conditions.

2.3. There may also be the added problem that applied AMB trial forces may not significantly show through in terms of trial responses, due to the dominance of the contact force magnitudes.

2.4. If the backward whirl mode becomes established, the high contact force magnitude and frequency may reach levels at which the required control action may exceed the load capacity of the AMB.

3.7. Active TDB options

The previous section has indicated that there may be occasions on which AMB control alone may not be able to restore contact-free rotor levitation. This leads to the consideration of making the TDB an active element. In Fig. 5, the displacement inputs to the TDB are (x_c, y_c). In the case of a passive TDB these would be set to zero, while for an active TDB, they would be determined by open or closed loop control strategies.

The issues that need to be addressed to bring an active TDB to fruition are:

3.1. The means of actuation such that TDB movement can be used effectively, while retaining the functionality required of a TDB i.e. preventing rotor/AMB stator contact.
3.2. The actuation force level requirements.
3.3. The sensor signals to be used for control purposes.
3.4. The control strategy to restore contact-free levitation.

Active TDB concepts are rare in the open literature. Ulbrich *et al*. [80, 81] considered the use of electromagnetic actuators, operating with relatively large strokes of 1 mm to move an auxiliary bearing. Their aim was to allow the rotor to enter a controlled rubbing condition, rather than contact-free levitation, in a manner that minimizes the contact force. If an active TDB were to be considered for use in an AMB system, the allowable TDB displacements would be much smaller than those considered in [80, 81]. For the example data presented in Table 1, a nominal rotor/TDB radial clearance of 0.5 mm could realistically allow an active TDB displacement of ±0.1 mm. This would enable the rotor/AMB gap to be maintained with a safety margin of 0.2 mm. A displacement of ±0.1 mm is within the performance limits of piezoelectric actuators, which can also have significant force capability. A prototype system has been designed and manufactured as described in [82]. The system is shown in Fig. 8. Direct coupling of the piezoelectric actuators to the TDB are avoided to protect against shear loads. The transmission of actuator force (up to 10 kN) and displacement (up to 0.1 mm) is achieved through the use of a closed hydraulic coupling, that is effective up to 800 Hz. The TDB is displaced using pairs of actuators in a push-pull configuration to reduce bearing distortion. Two orthogonal axes allow full 2D movement of the TDB in the axial plane. The signals that are available for control purposes include rotor speed, displacement, TDB displacement and actuator force. The TDB is directly coupled to an AMB that can deliver a maximum radial force of 2500 N with a current gain of 241 N/A. The PD controller gains were chosen to give a levitated rotor natural frequency of around 48 Hz (300 rad/s) with a damping ratio of 0.2. The integral gain is sufficiently low so as to have negligible influence at this frequency.

3.8. Active TDB control options

At present, the controller design is still an open question. A completely optimized closed loop controller would have to deal with the full range of non-linear contact dynamic behavior. Simple closed loop action could be configured to allow the effective stiffness and damping characteristics of the TDB mounting to be changed. However, this does not make full use of the active capability of the system. It is perhaps more useful to envisage monitoring of the rotor position relative to the TDB with a predictive capability for possible rotor/TDB contact. If rotor/TDB contact is anticipated, the TDB could be activated to maneuver in advance of a contact event and alleviate the contact force. In effect, the impulse of the contact event could be spread over a longer time interval, thus implying a lower maximum contact force. Further activation could be undertaken in an open-loop sense in a manner that

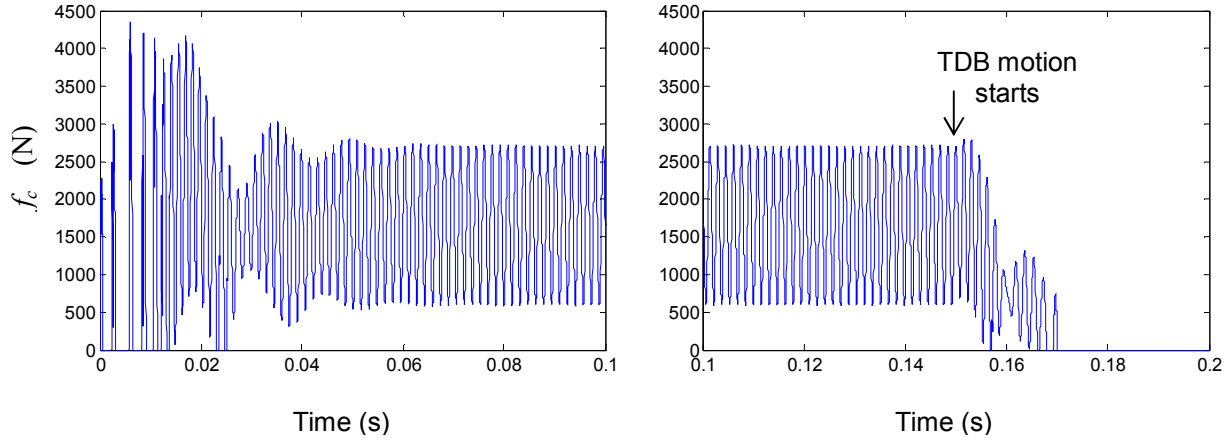

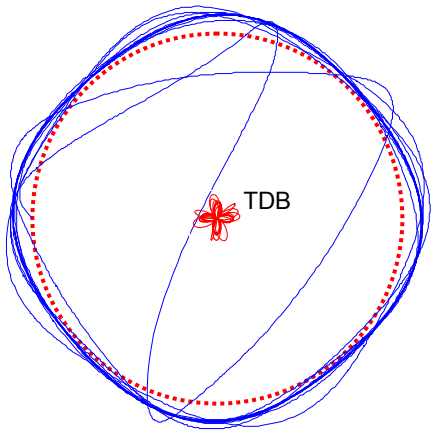

(x,y) rotor and TDB motions for 0 to 0.1 s showing initial contact to full rub

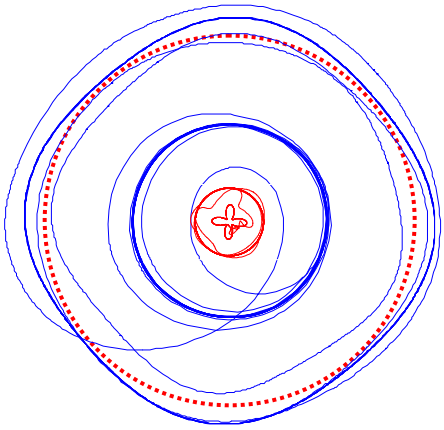

(x,y) rotor and TDB motions for 0.1 to 0.2 s showing full rub to loss of contact

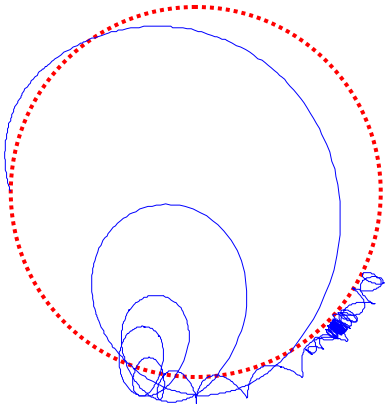

(u,v) rotor motion for 0 to 0.1 s

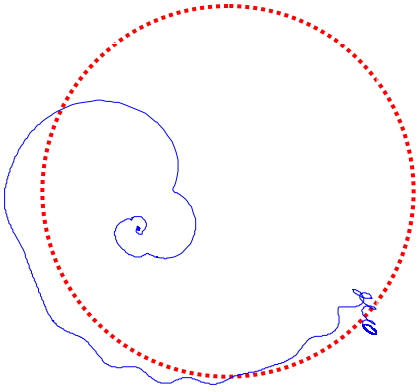

(u,v) rotor motion for 0.1 to 0.2 s

Fig. 9. Simulated contact force with rotor and TDB motions relative to nominal clearance circle, showing recovery of contact-free levitation after TDB open-loop actuation

destabilizes any trapped contact mode. This could be effective in terms of perceived clearance and reduced friction at the contact.

Under open-loop control it is possible to actuate the TDB so as to execute contact-free motions, for example,

$$x_b + iy_b = (\varepsilon_{bB} e^{-i(\Omega-\omega)t} + \varepsilon_{bF} e^{i(\Omega-\omega)t}) e^{i\varphi} \tag{48}$$

is a combination of non-synchronous backward and forward whirls. Practically, this is possible, though continuous operation of piezoelectric actuators may have significant power demands that lead to heating limitations. Hence it is envisaged that the open-loop control would be applied only on occasions when rotor/TDB contact is imminent.

Suppose that the rotor unbalance condition is such that the contact-free response would be a circular forward whirl orbit:

$$x_r + iy_r = \varepsilon_r e^{i(\Omega t - \vartheta)}, \quad \varepsilon_r < c_{rb} \tag{49}$$

In synchronously rotating coordinates the orbit becomes

$$u_r + iv_r = \varepsilon_r e^{-i\vartheta} \tag{50}$$

as represented by A in Fig. 7. If the TDB motion of (48) is imposed, the effective rotor/TDB gap will vary dynamically between $c_{rb} - \varepsilon_r \pm (\varepsilon_{bB} + \varepsilon_{bF})$. Without TDB motion, the residual gap before any contact is $c_{rb} - \varepsilon_r$.

Suppose that the rotor is in contact with the TDB is a forward circular synchronous rub mode:

$$x_r + iy_r = \varepsilon_{rb} e^{i(\Omega t - \varphi)}, \quad \varepsilon_{rb} > c_{rb} \tag{51}$$

If the TDB is in a passive state, an equilibrium condition for sustainable contact is

$$(-\Omega^2 + \omega_n^2 + 2i\xi\omega_n\Omega)\varepsilon_{rb} e^{-i\varphi} = e\Omega^2 - \frac{f_c}{m}(1 + i\mu) e^{-i\varphi} \tag{52}$$

The TDB could be controlled to execute a synchronous forward circular whirl orbit:

$$x_b + iy_b = (\varepsilon_{rb} - c_{rb}) e^{i(\Omega t - \phi)} \tag{53}$$

This will modify the equilibrium condition and if the phase is appropriately set, the rotor orbit may become unsustainable and contact-free levitation will return.

Simulated results for the data of Table 1 are shown in Fig. 9. The scenario is that a system disturbance has led the initial condition of rotor/TDB contact with the TDB centralized in a state of rest. An initial rotor orbit velocity of V = 0.3 m/s was selected with an angle of incidence at 135 deg with the TDB. Figure 9 shows the passive system response up to 0.15 s with the transition from the initial contact to a full rub condition. The bounce-like contacts, with contact forces up to 4500 N, eventually merge into continuous contact. The original unbalance force amplitude is 490 N, which causes a contact force with a mean value at 1650 N combined with a 4Ω oscillatory component of amplitude 1000 N. This is due to the non-isotropy of the AMB as the rotor passes the AMB pole faces. Significant TDB deflections are also evident. Note that the rotor weight is only 32 N, hence the

question that is raised is whether a standard rotor-drop test for a TDB would be a sufficient test to cope with the higher forces associated operational contact.

The feasibility of using an active TDB can be assessed in simulation. Figure 9 also shows the effect of applying open-loop actuator forces at 0.15 s to induce forward synchronous whirl of the TDB at around 20% of the radial clearance, after the full rub condition has become established. With appropriate phasing, the TDB motion is shown to cause a return to contact-free rotor levitation.

4. Conclusions

This paper has outlined some of the issues that should be considered to assess rotor dynamic behavior and ensure robust performance. Cases of weak and strong rotor dynamic coupling with contact events are covered. It is demonstrated how rotor dynamic design tools may be adapted to assess stability and rotor dynamic response.

The thermal bend problem is becoming familiar, though new and unexpected heat source examples are still being reported in the open literature. The methodology in this paper was undertaken in the transfer function domain to highlight the interaction between slow scale bend development and rotor dynamic response, considered to be non-synchronous. Analytical tools, based on matrix transfer function singular values, are available to provide stability boundaries.

The second part of the paper considered the stronger interaction case of contact in AMB systems. Here, contact forces may become high and vary between discrete and continuous rub events. If an AMB system remains operational, the contact dynamics will differ from those associated with the standard drop case. The options for using an active TDB to aid control of the contact rotor dynamics were also outlined.

Acknowledgement

The author acknowledges the support of the EPSRC through Grants EP/D031389 and GR/45277.

References

[1] American Petroleum Institute (API) Standard 684, Tutorial on the API Standard Paragraphs Covering Rotor Dynamics and Balance (An Introduction to Lateral Critical and Train Torsional Analysis and Rotor Balancing) (1996).

[2] ISO 14839-2:2004 Standard, Mechanical Vibration – Vibration of Rotating Machinery Equipped with Active Magnetic Bearings – Part 2: Evaluation of Vibration (2004).

[3] H.D. Taylor, Rubbing shafts above and below resonant speed, GE Technical Information Series, No. 16709 (1924).

[4] B.L. Newkirk, Shaft rubbing, Mechanical Engineering, Vol. **48**, No. 8 (1926), 830-832.

[5] R.P. Kroon, W.A. Williams, Spiral vibration of rotating machinery, Proc. 5th International Congress of Applied Mechanics, Wiley, New York (1939), 712-718.

[6] A.D. Dimarogonas, Newkirk effect: thermally-induced dynamic instability of high-speed rotors, International Gas Turbine Conference, Washington, D.C., April 1973, ASME Paper No. 73-GT-26.

[7] W. Kellenberger, Spiral vibrations due to the seal rings in turbogenerators: thermally-induced interaction between rotor and stator, Journal of Mechanical Design, Vol.**102** (1980), 177-184.

[8] J. Schmied, Spiral vibrations of rotors, ASME Design Technology Conference (Rotating Machinery Dynamics), Boston, Vol.**2** (1987), 449-456.

[9] P. Goldman, A. Muszynska, Rotor-to-stator, rub-related,thermal/mechanical effects in rotating machinery, Chaos, Solitons & Fractals, Vol.**5**(9) (1995), 1579-1601.

[10] J.T. Sawicki, A. Montilla-Bravo, Z. Gosiewski, Thermomechanical behavior of rotor with rubbing, International Journal of Rotating Machinery, Vol.**9**(1) (2003), 41-47.

[11] N. Bachschmid, P. Pennacchi, A. Vania, Thermally induced vibrations due to rub in real rotors, Journal of Sound and Vibration, Vol.**299** (2007), 683-719.

[12] L.Eckert, J. Schmied, A. Ziegler, Case history and analysis of the spiral vibration of a large turbogenerator using three different heat input models, 7th IFToMM Conference on Rotor Dynamics, Vienna, Austria, Sept. 2006.

[13] J. Schmied, J. Pozivil, J. Walch, Hot spots in turboexpander bearings: case history, stability analysis, measurements and operational experience, Paper GT2008-51179, ASME Turbo Expo, Berlin, Germany, June 2008.

[14] P.S. Keogh, P.G. Morton, Journal bearing differential heating evaluation with influence on rotor dynamic behaviour. Proc.R.Soc.Lond. A, Vol.**441** (1993), 527-547.

[15] P.S. Keogh, P.G. Morton, The dynamic nature of rotor thermal bending due to unsteady lubricant shearing within a bearing, Proc.R.Soc.Lond. A, Vol.**445** (1994), 273-290.

[16] R. Liebich, R. Gasch, Spiral vibrations - modal treatment of a rotor-rub problem based on coupled structural/thermal equations, Paper C500/042/96, Proc. 6th Int. Conf. Vibrations in Rotating Machinery, Oxford, UK, Sept. 1996, 405-413.

[17] R. Liebich, Rub Induced Non-Linear Vibrations Considering the Thermo-Elastic Effect, Proc. 5th IFToMM Conf. Rotor Dynamics, Darmstadt, Sept. 1998, 802-815.

[18] B. Larsson, Journal asymmetric heating - Part I: nonstationary bend, ASME J. Tribology, Vol.**121** (1999), 157-163.

[19] B. Larsson, Journal asymmetric heating - Part II: alteration of rotor dynamic properties, ASME J. Tribology, Vol.**121** (1999), 164-168.

[20] N. Bachschmid, P. Pennacchi, P. Venini, Spiral vibrations in rotors due to a rub, Paper C576/082/2000, Proc. 7th Int. Conf. Vibrations in Rotating Machinery, Nottingham, UK, Sept. 2000, 249-258.

[21] A.C. Balbahadur, R.G. Kirk, Part 1 - Theoretical model for a synchronous thermal instability operating in overhung rotors, International Journal of Rotating Machinery, Vol.**10**(6) (2004), 469-475.

[22] A.C. Balbahadur, R.G. Kirk, Part II - Case studies for a synchronous thermal instability operating in overhung rotors, International Journal of Rotating Machinery, Vol.**10**(6) (2004), 477-487.

[23] F.M. de Jongh, P.G. Morton, The synchronous instability of a compressor rotor due to bearing journal differential heating, Paper 94-GT-35, ASME Turbo Expo, The Hague, The Netherlands, June 2008.

[24] F. de Jongh, The synchronous rotor instability phenomenon - Morton effect, Proc. 37th Turbomachinery Symposium, Houston, USA, Sept. 2008.

[25] B.T. Murphy, J.A. Lorenz, Simplified Morton effect analysis for synchronous spiral instability, Paper POWER2009-81030, Proc. PWR2009 ASME Power, July 2009.

[26] T.M. Eldridge, A. Olsen, M. Carney, Morton-Newkirk effect in overhung rotor supported in rolling element bearings, Paper GT2009-60234, ASME Turbo Expo, Orlando, June 2009.

[27] D.C. Johnson, Synchronous whirl of a vertical shaft having clearance in one bearing, J. Mech. Eng. Sci., Vol.**4**(1) (1962), 85-93.

[28] F.F. Ehrich, Bistable vibrations of rotors in a bearing clearance. ASME Paper 65-WA/MD-1, 1965.
[29] H.F. Black, Interaction of a whirling rotor with a vibrating stator across a clearance annulus. J. Mech. Eng. Sci., Vol.**10**(1) (1968), 1-12.
[30] D.W. Childs, Rub induced parametric excitation in rotors. ASME J. Mechanical Design, Vol.**10** (1979), 640-644.
[31] D. Childs, Fractional-frequency rotor motion due to non-symmetric clearance effects, ASME J. Eng. Power, Vol.**104**(3) (1982), 533–541.
[32] A. Muszynska, Partial lateral rotor to stator rubs. Paper C281/84, Proc. 3rd Int. Conf. Vibrations in Rotating Machinery, York, UK, Sept. 1984, 327-335.
[33] F.F. Ehrich, High order subharmonic response of high speed rotors in bearing clearance, ASME J. Vibration, Acoustics, Stress and Reliability in Design, Vol.**110** (1988), 9-16.
[34] W. Zhang, Dynamic instability of multi-degree-of-freedom flexible rotor systems due to full annular rub, Paper C252/88, Proc. 4th Int. Conf. Vibrations in Rotating Machinery, Edinburgh, UK, Sept. 1988, 305-310.
[35] F.K. Choy, J. Padovan, J.C. Yu, Full rubs, bouncing and quasi chaotic orbits in rotating equipment, Journal of the Franklin Institute, Vol.**327** (1990), 25-47.
[36] Y.B. Kim, S.T. Noah, Bifurcation analysis for a modified Jeffcott rotor with a bearing clearance, Nonlinear Dynamics, Vol.**1** (1991), 221-241.
[37] J.L. Lawen, G.T. Flowers, Synchronous dynamics of a coupled shaft/bearing/housing system with auxiliary support from a clearance bearing. ASME J. Engineering for Gas Turbines and Power, Vol.**119** (1997), 430-435.
[38] S.-K. Choi, S.T. Noah, Mode-locking and chaos in a jeffcott rotor with bearing clearances, ASME Journal of Applied Mechanics, Vol.**61** (1994), 131-138.
[39] S. Popprath, H. Ecker, Nonlinear dynamics of a rotor contacting an elastically suspended stator, Journal of Sound and Vibration, Vol**.308** (2007), 767-784.
[40] H. Ecker, Nonlinear stability analysis of a single mass rotor contacting a rigid backup bearing, Dynamics of Vibro-Impact Systems (1999), 79-88.
[41] G. von Groll, D.J. Ewins, The harmonic balance method with arc-length continuation in rotor/contact problems, J. Sound and Vibration, Vol.**241** (2001), 223-233.
[42] A. Muszynska, Rotor-to-stationary part full annular contact modelling. Proc. 9th Int. Symp. Transport Phenomena and Dynamics of Rotating Machinery, Honolulu, Hawaii, Feb. 2002.
[43] M.O.T. Cole, On stability of rotordynamic systems with rotor–stator contact interaction, Proc.R.Soc.Lond. A, Vol.**464** (2008), 3353-3375.
[44] J. Schmied, J.C. Pradetto, Behavior of a one ton rotor being dropped into auxiliary bearings, Proc. 3rd Int. Symp. Magnetic Bearings, Alexandria, VA, July 1992, 145-156.
[45] R.G. Kirk, T. Ishii, Transient response drop analysis of rotors following magnetic bearing power outage, Proc. MAG'93, Alexandria, VA (1993), 53-61.
[46] R.G. Kirk, E.E, Swanson, F.H, Kavarana, X. Wang, Rotor drop test stand for AMB rotating machinery, Part 1: description of test stand and initial results, Proc. 4th Int. Symp. Magnetic Bearings, ETH Zurich, Aug. 1994, 207-212.
[47] E.E. Swanson, R.G., Kirk, J. Wang, AMB rotor drop initial transient on ball and solid bearings, Proc. MAG'95, Alexandria, VA (1995), 207-216.
[48] L. Hawkins, A. Filatov, S. Imani, D. Prosser, Test results and analytical predictions for rotor drop testing of an active magnetic bearing expander/generator, ASME J. Engineering for Gas Turbines and Power, Vol.**129** (2007), 522-529.

[49] M. Fumagalli, P. Varadi, G. Schweitzer, Impact dynamics of high speed rotors in retainer bearings and measurement concepts, Proc. 4th Int. Symp. Magnetic Bearings, ETH Zurich, Aug. 1994, 239-244.
[50] B.F. Feeny, Stability of cylindrical and conical motions of a rigid rotor in retainer bearings, Proc. 4th Int. Symp. Magnetic Bearings, ETH Zurich, Aug. 1994, 219-224.
[51] M. Fumagalli, G. Schweitzer, Measurements on a rotor contacting its housing. Paper C500/085/96, Proc. 6th Int. Conf. Vibrations in Rotating Machinery, Oxford, UK, Sept. 1996, 779-788.
[52] H. Ecker, Steady-state orbits of an AMB-supported rigid rotor contacting the backup bearings, Proc. MAG'97, Alexandria, VA (1997), 129-138.
[53] W.C. Foiles, P.E. Allaire, Nonlinear transient modeling of active magnetic bearing rotors during rotor drop on auxiliary bearings, Proc. MAG'97, Alexandria, VA (1997), 154-163.
[54] A.R. Bartha, Dry friction induced backward whirl: theory and experiment, Proc. 5th IFToMM Conf. Rotor Dynamics, Darmstadt, Sept. 1998, 756-767.
[55] X. Wang, S.T. Noah, Nonlinear dynamics of a magnetically supported rotor on safety auxiliary bearings. ASME J. Vibrations and Acoustics, Vol.**120** (1998), 596-606.
[56] R. Markert, G. Wegener, Transient vibration of elastic rotors in retainer bearings, Proc. ISROMAC-7, Hawaii, Feb. 1998, 764-774.
[57] G. Wegener, R. Markert, K. Pothmann, Steady-state-analysis of multi-disk and continuous rotors in retainer bearings, Proc. 5th IFToMM Conf. Rotor Dynamics, Darmstadt, Sept. 1998, 816-828.
[58] R.G. Kirk, Evaluation of AMB turbomachinery auxiliary bearings. ASME J. Vibrations and Acoustics, Vol.**121** (1999), 156-161.
[59] A.R. Bartha, Dry friction backward whirl of rotors, Doctoral Thesis, ETH, Zurich, 2000.
[60] J. Ji, L. Yu, Drop dynamics of a high-speed unbalanced rotor in active magnetic bearing machinery, Mech, Struct. Mach., Vol.**28** (2000), 185-200.
[61] J. Jiang, H. Ulbrich, Stability analysis of sliding whirl in a nonlinear Jeffcott rotor with cross-coupling stiffness coefficients, Nonlinear Dynamics, Vol.**24** (2001), 269-283.
[62] U. Ehehalt, R. Markert, Rotor motion during stator contact, Proc. 6th IFToMM Conf. Rotor Dynamics, Sydney, Sept. 2002, 913-920.
[63] E.N. Cuesta, V.R. , Rastelli, L.U. Medina, N.I. Montbrun, S.E. Diaz, Non-linear behaviors in the motion of a magnetically supported rotor on the catcher bearing during levitation loss, an experimental description, Paper GT-2002-30293, ASME Turbo Expo, Amsterdam, June 2002.
[64] P.S. Keogh, M.O.T. Cole, Rotor vibration with auxiliary bearing contact in magnetic bearing systems, Part I: synchronous dynamics, Proc. Instn Mech. Engrs, Part C, Vol.**217** (2003), 377-392.
[65] M.O.T. Cole, P.S. Keogh, Asynchronous periodic contact modes for rotor vibration within an annular clearance, Proc. Instn Mech. Engrs, Part C, Vol.**217** (2003), 1101-1115.
[66] M. Helfert, M. Ernst, R. Nordmann, B. Aeschlimann, High-speed video analysis of rotor-retainer-bearing-contacts due to failure of active magnetic bearings, Proc. 10th Int. Symp. Magnetic Bearings, Martigny, Switzerland, Aug. 2006.
[67] P. McMullen, V. Vuong, L. Hawkins, Flywheel energy storage system with AMB's and hybrid backup bearings, Proc. 10th Int. Symp. Magnetic Bearings, Martigny, Switzerland, Aug. 2006.
[68] M. Schlotter, P.S. Keogh, Synchronous position recovery control for flexible rotors in contact with auxiliary bearings, ASME Journal of Vibration and Acoustics, Vol.**129** (2007), 550-558.

[69] A. Kärkkäinen, J. Sopanen, A. Mikkola, Dynamic simulation of a flexible rotor during drop on retainer bearings, Journal of Sound and Vibration, Vol.**306** (2007), 601-617.

[70] L. Xie, M. Helfert, R. Nordmann, Numerical and experimental investigation of an AMB supported rotor system with auxiliary bearings, Proc. 9th Int. Conf. Vibrations in Rotating Machinery, Exeter, UK, Sept. 2008, 49-59.

[71] H.M. Chen, J. Walton, H. Heshmat, Test of zero clearance auxiliary bearing, Proc. MAG'97, Alexandria, VA (1997), 111-119.

[72] L.P. Tessier, The development of an auxiliary bearing landing system for a flexible AMB-supported hydrogen process compressor rotor, Proc. MAG'97, Alexandria, VA (1997), 120-128.

[73] Y. Ohura, K. Ueda, S. Sugita, Performance of touchdown bearings for turbo molecular pumps, Proc. 8th Int. Symp. Magnetic Bearings, Mito, Japan, Aug. 2002.

[74] T.W. Reitsma, Development of long-life auxiliary bearings for critical service turbomachinery and high-speed motors, Proc. 8th Int. Symp. Magnetic Bearings, Mito, Japan, Aug. 2002.

[75] M. Salehi, E. Swanson, H. Heshmat, Thermal features of compliant foil bearings – theory and experiments, ASME Journal of Tribology, Vol.**123** (2001), 566-571.

[76] G. Sun, A.B. Palazzolo, A. Provenza, G. Montague, Detailed ball bearing model for magnetic suspension auxiliary service, Journal of Sound and Vibration, Vol.**269** (2004), 933-963.

[77] G. Sun, A.B. Palazzolo, Rotor drop and following thermal growth simulations using detailed auxiliary bearing and damper models, Journal of Sound and Vibration, Vol.**289** (2006), 334-359.

[78] G. Sun, Auxiliary bearing life prediction using Hertzian contact bearing model, ASME J. Vibrations and Acoustics, Vol.**128** (2006), 203-209.

[79] P.S. Keogh, W.Y. Yong, Thermal assessment of dynamic rotor/auxiliary bearing contact events, ASME Journal of Tribology, Vol.**129** (2007), 143-152.

[80] H. Ulbrich, A. Chavez, R. Dhima, Minimization of contact forces in case of rotor rubbing using an actively controlled auxiliary bearing, Proc. 10th Int. Symp. Transport Phenomena and Dynamics of Rotating Machinery, Honolulu, Hawaii, March 2004, 1-10.

[81] H. Ulbrich, L. Ginzinger, Stabilization of a rubbing rotor using a robust feedback control, Paper-ID: 306, Proc. 7th IFToMM Conf. Rotor Dynamics, Vienna, Austria, 2006.

[82] I.S. Cade, M.N. Sahinkaya, C.R. Burrows, P.S. Keogh, On the design of an active auxiliary bearing for rotor/magnetic bearing systems, Proc. 11th Int. Symp. Magnetic Bearings, Nara, Japan, Sept. 2008.

[83] P.S. Keogh, M.N. Sahinkaya, C.R. Burrows, I.S. Cade, Rotor/auxiliary bearing dynamic contact modes in magnetic bearing systems, Proc. 11th Int. Symp. Magnetic Bearings, Nara, Japan, Sept. 2008.

[84] C.H. Cloud, W.F. Foiles, G. Li, E.H. Maslen, L.E. Barrett, Practical applications of singular value decomposition in rotordynamics, Proc. 6th IFToMM Conf. Rotor Dynamics, Sydney, Australia, Sept. 2002, 429-438.